

Experimental Research on a Split-Cathode-Fed Magnetron Driven by Long High-Voltage Pulses

G. Liziakin¹, O. Belozarov¹, J. G. Leopold², *Member, IEEE*, Yu. Bliokh¹, Y. Hadas, Ya. E. Krasik¹, *Fellow, IEEE*, and E. Schamiloglu², *Fellow, IEEE*

Abstract—In earlier research [Phys. Plasmas 27, 103102 (2020)], a split cathode was proposed to avoid pulse shortening of microwave generation in relativistic S-band magnetrons. Experiments confirmed the generation of microwave pulses limited only by the power generator's pulselength (~ 200 ns) [J. Appl. Phys. 131, 023301 (2022)]. In the current research, the results of experiments with the same magnetron but powered by a generator producing up to ~ 500 -ns-long high-voltage pulses are presented. It is shown that the power and duration of the microwaves depend strongly on the applied magnetic field, anode–cathode gap length, and the applied voltage amplitude. In the experiments, ~ 400 -ns, ~ 100 -MW microwave pulses were measured. It was also identified that impedance matching between the relativistic magnetron (RM) load and the high-voltage (HV) pulse generator is an important factor in the operation of these devices.

Index Terms—High-power microwaves (HPMs) generation, magnetrons, split-cathode-fed magnetron.

I. INTRODUCTION

SEVERAL decades of experimental research show that a relativistic magnetron (RM) can be considered as one of the most efficient high-power microwave (HPM) sources [1], [2], [3], [4], [5], [6], [7]. One of the problems that limit the power obtainable from an RM is pulse shortening. In [2], it is noted that HPM pulse shortening in rms occurs due to radial expansion of the cathode explosive emission plasma toward the anode. This can destroy the resonance condition between the

phase velocity of the electromagnetic wave and the electron drift velocity, resulting in an HPM pulse shorter than the applied voltage pulse duration. In [3], it was shown that the HPM pulse duration can be increased from ~ 100 to ~ 170 ns by preheating the cathode before the application of the high-voltage (HV) pulse. This results in less available expanding cathode plasma due to decrease in low-Z cathode surface contaminants. Another method to eliminate low-Z components is to coat a carbon fiber cathode with cesium iodide (CsI) [4]. In experiments with an L-band, 1.3-GHz RM using such cathodes, the HPM generation continued for ~ 450 ns, but these long HPM pulses were ≤ 20 -MW maximum power, compared to ~ 175 -MW, ≤ 100 -ns HPM pulses generated without CsI coating [4].

In order to minimize the influence of the expanding cathode plasma, Fuks [8] suggested to place an axial hollow cathode upstream from the RM anode and accelerate the electrons from the front of the plasma formed at the edge of the cathode toward the anode. The current of the electron beam magnetized by the external magnetic field is limited by the applied voltage and the radius of the tube coaxial to the cathode. This beam enters the anode and leaves it into a larger radius tube, which transmits a smaller current than that traversing the RM. This results in a virtual cathode formation at some distance from the end of the anode from which current is reflected upstream, leaving a leakage current flowing downstream [9]. Experiments [10], [11] confirmed HPM generation of up to 200-MW power and pulse duration of ~ 450 ns, but with an efficiency, $\leq 9\%$. Numerical simulations using magnetic mirrors to alleviate the leakage current in an RM with diffraction output (MDO) showed significantly increased efficiency up to 70% [12], [13], [14], [15]. However, the implementation of this idea in experiments is challenging.

Recently, another approach for external injection of the electron beam into the anode space was suggested [16]. Namely, a split cathode, which consists of a hollow cathode, placed outside and upstream of the RM anode block, connected to a reflector placed downstream from the anode by a conducting central rod. Electrons emitted from the cathode plasma oscillate between the cathode and the reflector. These electrons with potential energy smaller than the cathode–anode (C–A) potential difference gradually fill the potential well

Manuscript received 17 October 2023; revised 6 December 2023 and 19 December 2023; accepted 2 January 2024. Date of publication 17 January 2024; date of current version 1 March 2024. This work was supported in part by the Technion under Grant 2029541, in part by Office of Naval Research Global (ONRG) Grant N62909-21-1-2006, and in part by The University of New Mexico through Office of Naval Research (ONR) under Grant N00014-23-1-2072. The review of this article was arranged by Editor E. Choi. (Corresponding author: G. Liziakin.)

G. Liziakin, O. Belozarov, J. G. Leopold, Yu. Bliokh, Y. Hadas, and Ya. E. Krasik are with the Department of Physics, Technion–Israel Institute of Technology, Haifa 3200003, Israel (e-mail: gennadii@technion.ac.il).

E. Schamiloglu is with the Department of Electrical and Computer Engineering, The University of New Mexico, Albuquerque, NM 87131 USA (e-mail: edls@unm.edu).

Color versions of one or more figures in this article are available at <https://doi.org/10.1109/TED.2024.3350563>.

Digital Object Identifier 10.1109/TED.2024.3350563

formed between the cathode-rod-reflector and the anode. For high magnetic fields, the well fills up with a charge, electrons kinetic energy decreases, and finally, a squeezed state of the accumulated electrons can be obtained [17]. Recent studies of the split-cathode-fed RM [18], [19], [20] confirm that this approach can be successfully used for HPM generation. It was demonstrated that this RM generates ~ 200 -ns-long HPM pulses corresponding to the duration of the HV pulse. For the same conditions, a solid cathode underwent pulse shortening at ~ 120 ns.

Although HPM pulse shortening is usually associated with the cathode plasma expansion and shorting of the C–A gap, centrifugal plasma instability can also be responsible for it. In experiments (i.e., [21]), HPM pulse shortening occurs, while the voltage is still on, which means that the plasma's radial expansion does not short the C–A gap but only decreases it. The smaller plasma boundary–anode gap causes a mismatch between the electron drift velocity and the wave's phase velocity and leads to the termination of HPM generation. In fact, the decrease in the gap width can lead to an increase in the electron current toward the anode causing the pulse power generator's voltage to drop and consequently a reduced applied voltage on the C–A gap. Thus, the impedance matching of the RM and the generator is an important issue [22], [23].

In a split-cathode-fed RM, inside the anode interaction space, there are only oscillating electrons. The electron space charge accumulates there and expands radially due to Coulomb repulsion. During this process, diocotron instabilities can develop [24]. This can also lead to increase in the current toward the anode, resulting in RM and generator impedance mismatch and termination of HPM generation. In addition, the external cathode explosive emission plasma expands toward the anode along the magnetic field lines with a velocity of $\sim 10^7$ cm/s [25]. This leads to the decrease in the axial gap between the plasma and the anode, an increase in the emitted current, and a voltage decrease due to the generator finite impedance. All this can result in a change in the RM operating conditions and to the cessation of the microwave power. If the HV generator provides a long pulse, this cessation of power could be temporary and new conditions for HPM generation may recur intermittently.

The purpose of the present article is to test HPM generation using a split-cathode-fed RM for long applied HV pulses. In the present study, a pulsed power generator supplies ~ 500 -ns-long HV pulses for the same split-cathode-fed axial output RM as that used in previous research [19], [20]. The results of these experiments show that for these conditions, this RM generates intermittent HPM radiation with pulse duration up to ~ 400 ns for a C–A distance of 2.5 cm.

II. EXPERIMENTAL SETUP

In the split-cathode-fed segmented anode RM, the external solenoid and its power supply used in the present research (see Fig. 1) are the same as in earlier studies [19], [26]. The RM was supplied by a 20-stage HV Marx generator with an internal impedance of $\sim 50 \Omega$. Each stage is a pulse-forming network (PFN) consisting of four low-inductance capacitors (50 nF, 50 kV) connected in parallel. The Marx generator

was operated at charging voltages in the range 12–35 kV, which result in maximal voltage amplitudes applied to the RM in the range 150–350 kV with pulse durations ~ 200 –500 ns depending on the RM impedance.

The aluminum RM anode is 60 mm long with inner and outer radii of 21 and 42 mm, respectively. The anode is placed in a cylindrical tube, followed by a closed conical section (see Fig. 1). Three 2-mm-wide angular slits cut radially along the three lines seen in Fig. 1(c) allow the external magnetic field's fast penetration. The design of the extraction of the microwaves transforms the axial output into a TM_{01} waveguide mode, which serves as the input to a 17-dB gain conical antenna [20].

The split cathode consists of 5-mm-long carbon capillaries fixed in 18-mm-diameter aluminum cathode and symmetrically distributed azimuthally along a 12-mm-diameter circle [19]. Upstream from the cathode, a 40-mm-diameter reflector is placed. The axial distance between reflector 1 and the edge of the capillaries is denoted as d_{R1-C} . The axial distance between the upstream edge of the anode and the edge of the capillaries, d_{C-A} can be varied in the range 10–47 mm. A second 40-mm-diameter downstream aluminum reflector is connected to the upstream cathode reflector 1 by a 6-mm-diameter aluminum rod. The axial distance between reflector 2 and the downstream edge of the anode d_{A-R2} is chosen to be the same as d_{C-A} . The RM structure is housed within a 400-mm-long Perspex tube, where the vacuum $3 \cdot 10^{-2}$ Pa is maintained by a turbomolecular pump. At the downstream end of the system, a conical antenna covered with a Perspex window is attached to the output of the RM.

An external solenoid consisting of a single copper wire layer is wound around the Perspex tube. The solenoid is energized by a current pulse of a few kiloamperes, 90- μ s half-period produced by the discharge of a 25- μ F capacitor charged to a voltage ranging from 2.3 to 7.5 kV. The solenoid produces a magnetic field in the range $B = 0.15$ –0.5 T with axial distribution shown in Fig. 1(b). A resistive voltage divider placed at the output of the Marx generator was used to measure the voltage. The total current was measured by a Rogowski coil placed upstream from the solenoid [see Fig. 1(a)]. The microwave electric field was measured by a D-dot sensor SFE-10G (Montena) equipped with a PROLYN Balun BIB-100G. The electric field E [V/m] was calculated as: $E = U_d 10^{k/20} / 2\pi f \epsilon_0 Z S$, where f is the microwave frequency, ϵ_0 is the dielectric constant of free space, $Z = 50 \Omega$ is the balun impedance, $S = 2 \times 10^{-4} \text{ m}^2$ is the D-dot dipole cross section area, V_d is the voltage of the microwave signal registered by an Agilent Infiniium DSO 54855a oscilloscope, and k is the total attenuation coefficient in dB. The spatial distribution of the microwave power in the horizontal or vertical polarization of the D-dot sensor was measured at a distance of 150 cm from the output window of the radiating antenna. These measurements reveal that the spatial distributions for both vertical and horizontal polarizations are almost identical. Considering that the power flux density is related to the electric field as: E [V/cm] = $19(P[W/cm^2])^{1/2}$ [27], the total power density was calculated as the sum of the power densities for each electric field polarization.

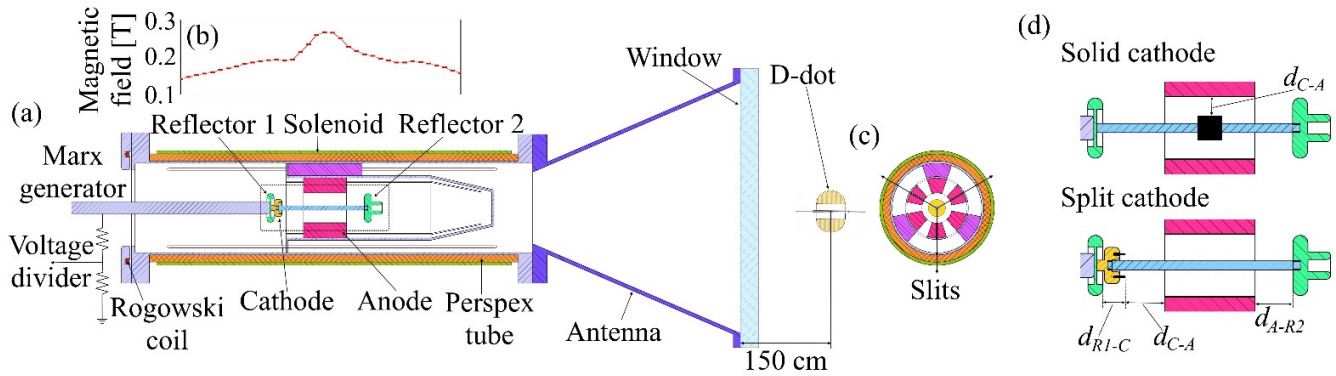


Fig. 1. (a) Longitudinal cross section of the experimental setup. (b) Axial magnetic field distribution for 4-kV charging voltage of the solenoid's pulsed power supply. (c) Black arrows in the azimuthal cross section at the RM center indicate the position of the three longitudinal slots separating the anode into segments. (d) Cross sections of the RM with solid and split cathodes.

III. EXPERIMENTAL RESULTS

In Fig. 2, one can see the waveforms of the RM voltage, current, and the microwave electric field for four values of the applied magnetic field and two values of the charging voltage.

First, note that for all cases, the current does not exceed a few hundred amperes during the first ~ 50 ns as the voltage increases. This is typical for a split cathode due to small net current during the electron charge accumulation between the two reflectors. When the space charge becomes sufficiently large, the electron cloud expansion leads to the appearance of anode current. A drop of the voltage to zero before the end of the generated microwave pulse, which would indicate that the cathode plasma shorts the C-A gap, was not observed in any of the cases shown in Fig. 2 or in any of our other experiments. This means that the HPM pulse seen in Fig. 2(c) terminates not because of plasma shorting but due to other possible mechanisms mentioned in Section I. For the highest magnetic field considered in Fig. 2(e) at $\varphi_{ch} = 20$ kV, the microwave pulse is relatively long, ~ 300 ns. The longest microwave pulse (~ 400 ns) was obtained for $\varphi_{ch} = 25$ kV and $B_z = 0.4$ T [Fig. 2(f) and (g)]. In all cases seen in Fig. 2, when long radiated microwave pulses are observed, these are characterized by intermittent modulation of the amplitude and varying frequency [Fig. 2(b), (f), and (h)]. For the long duration (~ 300 ns) HPM pulse with $B_z = 0.37$ T [Fig. 2(e)], the intermittent behavior can be related to switching between different modes [Fig. 2(f)], while the frequency changes in intermittent intervals between 1.9 and 2.1 GHz. The frequency changes in a similar way in Fig. 2(h). For the lower magnetic fields [0.27 T in Fig. 2(d) and 0.18 T in Fig. 2(b)], the most pronounced frequency feature is a drift from 1.85 to 1.7 GHz in the main part of the microwave pulse.

For comparison, similar experiments were carried out with a solid cathode. The solid cathode was a 16-mm-long, 16-mm-diameter carbon rod with 12 1-mm-deep azimuthally distributed longitudinal grooves. This cathode was placed along the axis at the center of the anode, and reflectors #1 and #2 (Fig. 1) were placed at a distance of 25 mm from the anode edges. The performance of the solid cathode fed RM was qualitatively similar to that with the split cathode. For example, with two different charging voltages, results are presented in Fig. 3 for $B_z = 0.38$ T. Fig. 3(c) is for the conditions that the

longest HPM pulse was obtained, that is, ~ 200 -ns, ~ 50 -kV/m maximum amplitude, ~ 30 -MW peak power. The solid cathode's radial distance to the anode (1.3 cm) is significantly smaller than the distance of the external annular cathode to the magnetron anode block (2.5 cm) for the split cathode. For the solid cathode, the plasma's radial expansion transverse to the magnetic field direction is slower than the axial plasma expansion along the direction of the magnetic field for the split cathode [25]. Thus, the plasma radial expansion for a solid cathode has a stronger effect on RM operation than the external plasma's axial expansion together with the internal electron cloud's radial expansion for the split cathode. Note that the axial plasma velocity depends strongly on the emitted current density from its front [25].

In Fig. 4, the microwave pulses obtained with a split cathode for the same geometric parameters as in Fig. 2 and for $B_z = 0.177$ – 0.4 T are shown. The Hull cutoff (HC) seems to be slightly below $B_z = 0.177$ T, and by 0.5 T, no microwaves are produced. Then, intermittency in the time dependence of the microwave pulses and pulse lengths of ~ 350 ns at 0.38 T but with overall intermissions of over ~ 100 ns was obtained. Apart from the intermittency, the increase in the time delay at the onset of microwave generation seen in Fig. 4 is similar to the results of PIC simulations ([24, Figs. 11 and 12] and the corresponding discussion). Note that the time delay between the voltage beginning ($t = 0$) and that of the microwaves increases in the region 0.177–0.26 T from ~ 20 to ~ 35 ns. At the same time, the maximum amplitude of the microwave electric field increases from ~ 42 to ~ 80 kV/m. In this range of low to intermediate magnetic fields, following [24], RM operation depends only weakly on the axial electron oscillations. Within this region, there are amplitude variations, there is no significant intermittency, and the HPM pulse duration is relatively short due to electron cloud expansion. At 0.33 T, the time delay increases considerably to ~ 60 ns and the maximum electric field reduces to ~ 50 kV/m. From this point on and up to 0.4 T, the maximum amplitude increases to ~ 80 kV/m and intermittencies set in. In this region, Leopold et al. [24] predict that partial squeezing starts to affect the dynamics and changes in the resonant mode appear.

In the PIC simulations (see [24]), no intermittency was observed because two processes were ignored. Plasma

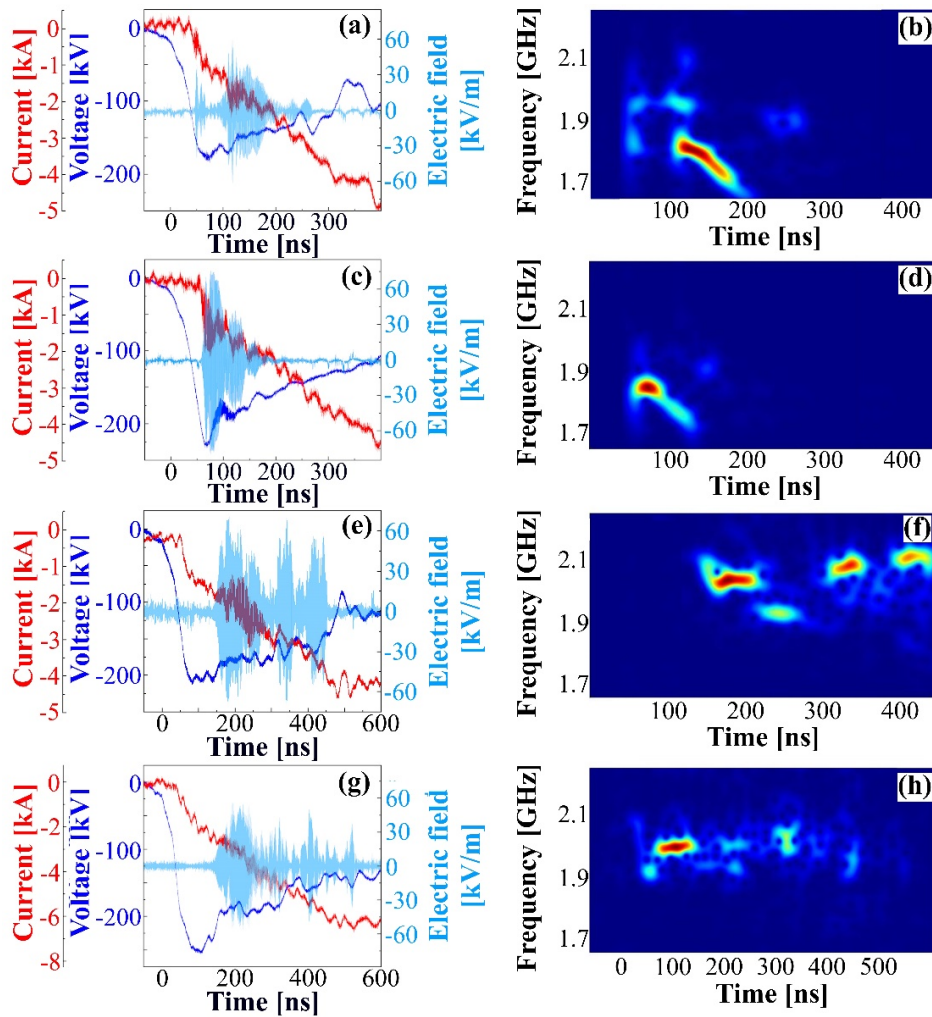


Fig. 2. (a), (c), (e), and (g) Waveforms of the current, voltage, and microwave electric field. (b), (d), (e), and (h) Time–frequency analysis for $d_{c-A} = 25$ mm, $d_{R1-C} = 42$ mm, and $\phi_{ch} = 20$ kV. (a) and (b) $B_z = 0.18$ T. (c) and (d) 0.27 T. (e) and (f) 0.37 T. The longest microwave pulse observed at $\phi_{ch} = 25$ kV. (g) and (h) $B_z = 0.4$ T.

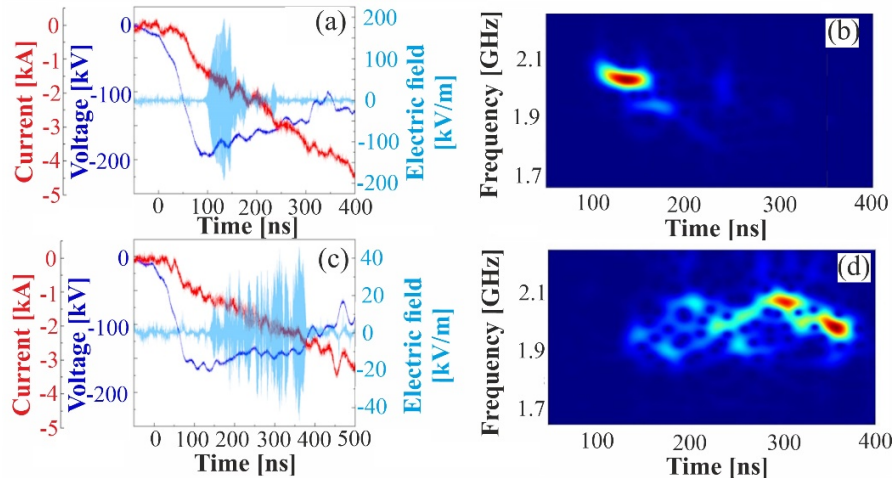


Fig. 3. (a) and (c) Waveforms of the current, voltage, and microwave electric field. (b) and (d) Time–frequency analysis for a 16-mm-diameter, 16-mm-long solid cathode. (a) and (b) $B_z = 0.38$ T and $\phi_{ch} = 20$ kV. (c) and (d) $\phi_{ch} = 15$ kV.

expansion is not included, and the presence of the generator as a circuit attached to the transmission line feeding is also neglected. In the experiments, a change in the RM current changes the voltage applied to the RM due to the generator's finite impedance. These effects are usually neglected in most

simulations in the literature, but as seen here, the generator impedance has a serious effect [22], [23].

It was stated in [24] that the ordinary HC and Buneman–Hartree (BH) limits cannot be applied directly to a split-cathode-fed RM because of the presence of axial

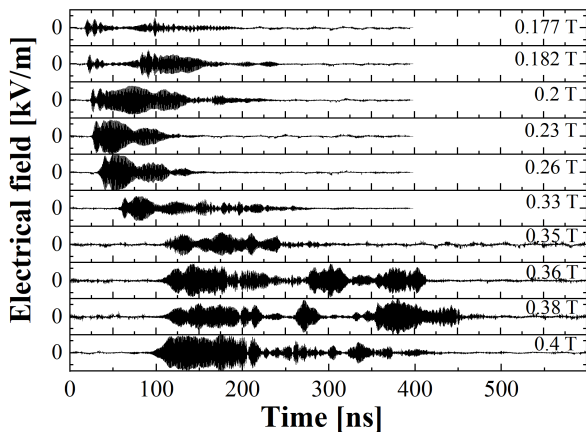


Fig. 4. Microwave electric field component measured on axis at a distance of 1.5 m from the RM for different values of the magnetic field for the same conditions as in Fig. 2(a)–(f). Vertical scale for each electric field curve is 50 kV/cm/div.

electron oscillations with time-dependent energy even for a fixed applied voltage. Also, the electrons being generated at cathode potential outside the anode enter the anode interior at a higher potential value than electrons emitted from a coaxial cathode. In addition, for a given value of ϕ_{ch} , the voltage decreases during microwave generation when the current increases. The RM is a nonlinear load whether fed by a solid or split cathode, and its voltage to current relation depends on the finite impedance of the Marx generator. For long pulse generators, the temporal changes in the generator voltage can result in intermittent microwave generation.

Nevertheless, one can consider that the obtained experimental results relate to the HC and BH limits calculated for electrons entering the anode at the radius of the outer cathode's emitting circle. In Fig. 5, the BH limits for three possible modes are drawn in bands of frequencies as a typical voltage versus magnetic field plot. The results were combined in four groups of microwave pulse lengths represented in Fig. 5 by the size of the corresponding circles. The experiments were carried out at three different charging voltages, 12.5, 20, and 25 kV. These are drawn using three different colors. A higher charging voltage corresponds to greater generator energy applied to the RM. Because of impedance mismatch, plasma, and electron cloud expansion, the dependence of the C–A voltage and current on the charging voltage is complex. The vertical bars in Fig. 5 mark the voltages at the beginning and end of the microwave pulse. As the microwave pulselength increases, intermittency increases as well, as shown in Fig. 4. Long and short pulses can appear at the same or nearly the same magnetic field for different charging voltages. One should note, though, that the three regions of magnetic field values mentioned above are clearly discernible in Fig. 5. For magnetic fields up to ~ 0.3 T, the experimental data concentrate near the π mode area and most of the microwave pulses are 100–200 ns long. Microwave pulses in the transition from the π - to 2π -mode region which appear for $0.3 \text{ T} \leq B_z < 0.35 \text{ T}$ are long but intermittent.

The dependence of the maximum power of the HPM pulse on magnetic field at a charging voltage of 20 kV is presented in Fig. 6. For magnetic fields increasing up to ~ 0.25 T, the

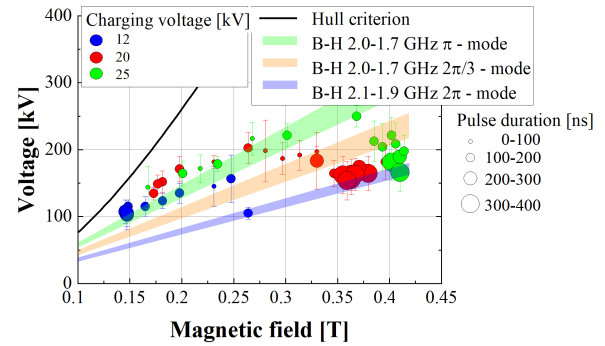


Fig. 5. Position of the experimental shots on common Hull–Buneman–Hartree diagram at $d_{R1-C} = 42$ mm and $d_{C-A} = 25$ mm. Circle size represents MW pulse duration, and vertical bar indicates voltage variation during microwave generation.

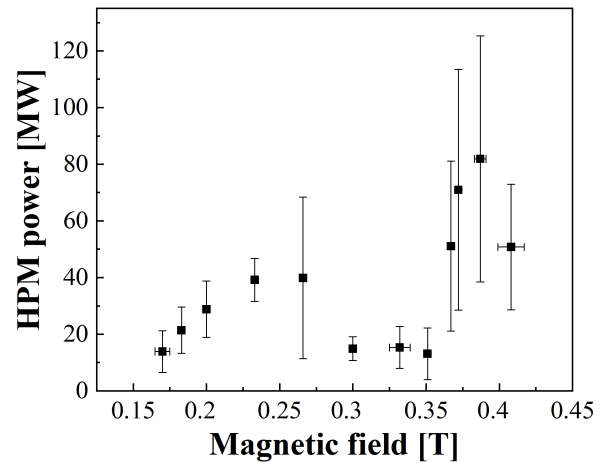


Fig. 6. Dependence of the maximum power of the HPM pulse versus magnetic field at $\phi_{ch} = 20$ kV, $d_{C-A} = 25$ mm, and $d_{R1-C} = 42$ mm.

power increases to a level of ~ 40 MW for relatively short pulses. Then, for $B_z > 0.35$ T, the maximum power can reach ~ 80 MW over intermittent long pulses. Similar dependencies were obtained for other tested values of d_{C-A} .

When the distance d_{R1-C} between the upstream reflector and cathode is reduced from 42 to 22 mm (at $d_{C-A} = d_{A-R2} = 25$ mm), then for high magnetic fields ($B_z > 0.35$ T), the duration of the intermittent pulses decreases from 400 to 300 ns and the maximal power increases from ~ 80 up to ~ 170 MW. One can suppose that when the distance between the reflectors is reduced, the electron time-of-flight between the reflectors decreases, so that at high magnetic fields, the synchronization between the axial oscillations and the RM eigenmode becomes more important.

When the distance d_{C-A} increases from 25 to 47 mm, there is no significant change in the HPM pulse duration and power. It means that for these relatively large C–A distances, the cathode plasma's axial expansion does not influence the parameters of the HPM pulse. Decreasing d_{C-A} from 25 to 10 mm ($B_z > 0.35$ T, $d_{R1-C} = 22$ mm) decreases the pulse duration from 300 to 120 ns, while the maximal power increases from 170 to 400 MW. For this value of $d_{C-A} = 10$ mm, the amplitude of the voltage decreases below 100 kV within ~ 215 ns when the microwave generation vanished also for other tested values of d_{C-A} . Thus, even for $d_{C-A} = 10$ mm,

the termination of microwaves generation does not related to the shorting of the A–C gap by the axially expanding cathode plasma.

To conclude, the longest intermittent HPM pulses (~ 400 ns) were obtained for $\phi_{\text{ch}} = 25$ kV, $B = 0.4$ T, $d_{c-A} = 25$ mm, and $d_{R1-C} = 42$ mm. On the other hand, a maximum power of ~ 400 MW but with a duration of ~ 120 ns was registered for $\phi_{\text{ch}} = 20$ kV, $B = 0.38$ T, $d_{c-A} = 10$ mm, and $d_{R1-C} = 22$ mm.

IV. CONCLUSION

For all parameters varied in this study of the split-cathode-fed RM attached to a long pulse generator, the HPM pulses were shorter than the duration of the generator pulse. Pulse shortening interruption caused by plasma short circuit of the C–A gap was not obtained even for cathodes as close as 1 cm from the anode. For relatively high magnetic fields, long HPM pulses appeared intermittently over time, and their maximum power was usually higher than for the lower magnetic field region, where the pulses were shorter, less intermittent, and the power increases with increasing magnetic field just as one would expect the behavior between the HC and BH limits. Increasing the magnetic field seems to be connected with an RM mode change, confirmed by our earlier simulations [24].

In the case of solid cathodes, short-circuit cases were also not obtained. HPM pulse shortening was caused by plasma expansion in the coaxial gap, but a similar behavior was obtained with the split cathode related to the effect of the change in the gap width on the generator voltage and current. Overall, a solid cathode produces shorter pulses and lower power for the same parameter region as that studied for the split cathode.

The results of this experimental study of a split-cathode-fed RM powered by a long duration HV pulse showed three different modes of its operation with low (<0.22 T), intermediate, and high (>0.35 T) magnetic fields. These modes differ in duration and power of HPM pulse, as well as in the stability of the frequency during microwave generation. The latter indicates on mode competition, which can be related to the change in the amplitude of the HV pulse as well as to the dynamics of the oscillating electrons.

REFERENCES

- [1] D. Andreev, A. Kuskov, and E. Schamiloglu, "Review of the relativistic magnetron," *Matter Radiat. Extremes*, vol. 4, no. 6, Oct. 2019, Art. no. 067201, doi: [10.1063/1.5100028](https://doi.org/10.1063/1.5100028).
- [2] J. Benford and G. Benford, "Survey of pulse shortening in high-power microwave sources," *IEEE Trans. Plasma Sci.*, vol. 25, no. 2, pp. 311–317, Apr. 1997, doi: [10.1109/27.602505](https://doi.org/10.1109/27.602505).
- [3] D. Price, J. S. Levine, and J. N. Benford, "Diode plasma effects on the microwave pulse length from relativistic magnetrons," *IEEE Trans. Plasma Sci.*, vol. 26, no. 3, pp. 348–353, Jun. 1998, doi: [10.1109/27.700765](https://doi.org/10.1109/27.700765).
- [4] B. A. Kerr, "Carbon velvet cathode implementation on the Orion relativistic magnetron," in *Proc. IEE Pulsed Power Symp.*, Basingstoke, U.K., 2005, pp. 1–6, doi: [10.1049/ic:20050035](https://doi.org/10.1049/ic:20050035).
- [5] V. L. Granatstein and I. Alexeff, *High-Power Microwave Sources*. Boston, MA, USA: Artech House 1987, p. 369.
- [6] T. A. Treado, "Generation and diagnosis of long- and short-pulse, high-power microwave radiation from relativistic rising sun and A6 magnetrons," Ph.D. dissertation, Dept. Phys., North Carolina State Univ., Raleigh, NC, USA, 1989.
- [7] D. Price and J. N. Benford, "General scaling of pulse shortening in explosive-emission-driven microwave sources," *IEEE Trans. Plasma Sci.*, vol. 26, no. 3, pp. 256–262, Jun. 1998, doi: [10.1109/27.700752](https://doi.org/10.1109/27.700752).
- [8] M. I. Fuks, "Investigation of electronics flows in magnetically insulated sources," Ph.D. dissertation, Inst. Appl. Phys., Nizhny Novgorod, Russia, 1983.
- [9] B. N. Brejzman and D. D. Ryutov, "Powerful relativistic electron beams in a plasma and in a vacuum (theory)," *Nucl. Fusion*, vol. 14, no. 6, pp. 873–907, Dec. 1974, doi: [10.1088/0029-5515/14/6/012](https://doi.org/10.1088/0029-5515/14/6/012).
- [10] L. F. Chernogalova et al., "Experimental investigations of the magnetically insulated diode and microwave generation in the relativistic magnetrons," in *Proc. 6th Int. Conf. High Power Electron Ion Beam Res. Technol.*, 1986, pp. 573–576.
- [11] I. I. Ventizenko, N. F. Kovalev, A. S. Sulakshin, G. P. Fomenko, and M. I. Fuks, *Proceedings of the V All-Union Seminar on Relativistic High-Frequency Electronics*. Novosibirsk, Russia. Nizhny Novgorod, Russia: Inst. Appl. Phys., Nov. 1987, pp. 125–140.
- [12] M. I. Fuks, S. Prasad, and E. Schamiloglu, "Efficient magnetron with a virtual cathode," *IEEE Trans. Plasma Sci.*, vol. 44, no. 8, pp. 1298–1302, Aug. 2016, doi: [10.1109/TPS.2016.2525921](https://doi.org/10.1109/TPS.2016.2525921).
- [13] A. V. Gromov, M. B. Goykhan, N. F. Kovalev, A. V. Palitsin, M. I. Fuks, and E. Schamiloglu, "The low-energy state of an electron beam in a coaxial diode with a homogeneous anode and inhomogeneous magnetic field profile," *Tech. Phys. Lett.*, vol. 44, no. 10, pp. 949–952, Dec. 2018, doi: [10.1134/S1063785018100243](https://doi.org/10.1134/S1063785018100243).
- [14] E. Schamiloglu, M. I. Fuks, A. A. Koronovskii, and S. A. Kurkin, "Efficient relativistic magnetron with lengthy virtual cathode formed using the magnetic mirror effect," in *Proc. IVEC*, London, U.K., 2017, pp. 1–2, doi: [10.1109/IVEC.2017.8289558](https://doi.org/10.1109/IVEC.2017.8289558).
- [15] M. I. Fuks and E. Schamiloglu, "Application of a magnetic mirror to increase total efficiency in relativistic magnetrons," *Phys. Rev. Lett.*, vol. 122, no. 22, Jun. 2019, Art. no. 224801, doi: [10.1103/PhysRevLett.122.224801](https://doi.org/10.1103/PhysRevLett.122.224801).
- [16] J. G. Leopold, Y. E. Krasik, Y. P. Bliokh, and E. Schamiloglu, "Producing a magnetized low energy, high electron charge density state using a split cathode," *Phys. Plasmas*, vol. 27, no. 10, Oct. 2020, Art. no. 103102, doi: [10.1063/5.0022115](https://doi.org/10.1063/5.0022115).
- [17] Y. Bliokh, J. G. Leopold, and Y. E. Krasik, "Squeezed state of an electron cloud as a 'quasi-neutral' one-component plasma," *Phys. Plasmas*, vol. 28, no. 7, Jul. 2021, Art. no. 072106, doi: [10.1063/5.0056881](https://doi.org/10.1063/5.0056881).
- [18] J. G. Leopold et al., "Experimental and numerical study of a split cathode fed relativistic magnetron," *J. Appl. Phys.*, vol. 130, no. 3, Jul. 2021, Art. no. 034501, doi: [10.1063/5.0055118](https://doi.org/10.1063/5.0055118).
- [19] Y. E. Krasik et al., "An advanced relativistic magnetron operating with a split cathode and separated anode segments," *J. Appl. Phys.*, vol. 131, no. 2, Jan. 2022, Art. no. 023301, doi: [10.1063/5.0080421](https://doi.org/10.1063/5.0080421).
- [20] O. Belozero et al., "Characterizing the high-power-microwaves radiated by an axial output compact S-band A6 segmented magnetron fed by a split cathode and powered by a linear induction accelerator," *J. Appl. Phys.*, vol. 133, no. 13, Apr. 2023, Art. no. 133301, doi: [10.1063/5.0138769](https://doi.org/10.1063/5.0138769).
- [21] Y. M. Saveliev, B. A. Kerr, M. I. Harbour, S. C. Douglas, and W. Sibbett, "Operation of a relativistic rising-sun magnetron with cathodes of various diameters," *IEEE Trans. Plasma Sci.*, vol. 30, no. 3, pp. 938–946, Jun. 2002, doi: [10.1109/TPS.2002.801652](https://doi.org/10.1109/TPS.2002.801652).
- [22] J. G. Leopold, A. S. Shlapakovski, A. Sayapin, and Y. E. Krasik, "Revisiting power flow and pulse shortening in a relativistic magnetron," *IEEE Trans. Plasma Sci.*, vol. 43, no. 9, pp. 3168–3175, Sep. 2015, doi: [10.1109/TPS.2015.2463717](https://doi.org/10.1109/TPS.2015.2463717).
- [23] J. G. Leopold, A. S. Shlapakovski, A. F. Sayapin, and Y. E. Krasik, "Pulse-shortening in a relativistic magnetron: The role of anode block axial endcaps," *IEEE Trans. Plasma Sci.*, vol. 44, no. 8, pp. 1375–1385, Aug. 2016, doi: [10.1109/TPS.2016.2580613](https://doi.org/10.1109/TPS.2016.2580613).
- [24] J. G. Leopold, Y. Bliokh, Y. E. Krasik, A. Kuskov, and E. Schamiloglu, "Diocotron and electromagnetic modes in split-cathode fed relativistic smooth bore and six-vane magnetrons," *Phys. Plasmas*, vol. 30, no. 1, Jan. 2023, Art. no. 013104, doi: [10.1063/5.0129515](https://doi.org/10.1063/5.0129515).
- [25] S. P. Bugaev, V. I. Kanavez, V. I. Koshelev, and V. A. Cherepinin, *Relativistic Multi-Wave Microwave Generators*. Novosibirsk, Russia: Nauka, Siberian Branch, 1991.
- [26] J. G. Leopold, Ya. E. Krasik, Y. Hadas, and E. Schamiloglu, "An axial output relativistic magnetron fed by a split cathode and magnetically insulated by a low-power solenoid," *IEEE Trans. Electron Devices*, vol. 68, no. 10, pp. 5227–5231, Oct. 2021, doi: [10.1109/TED.2021.3105942](https://doi.org/10.1109/TED.2021.3105942).
- [27] Y. P. Raizer, *Gas Discharge Physics*. Berlin, Germany: Springer, 2011.